ADVANCED ENGINEERING MATERIALS

DOI: 10.1002/adem.200900052

Spark Plasma Sintering as a Useful Technique to the Nanostructuration of Piezo-Ferroelectric Materials**

By *Teresa Hungría**, *Jean Galy* and *Alicia Castro*

This review gathers detail on the processing of piezo-ferroelectric ceramic materials by spark plasma sintering for the first time. The results reported here clearly indicate that it is a powerful technique and opens the possibility of processing ceramics with controlled sub-micron or even nanoscale grain sizes.

1. Introduction

Piezoelectric and ferroelectric ceramic materials are mature and ubiquitous materials for advanced technology. These ceramics are the active elements in a range of piezoelectric devices and perform functions such as sensing and actuation. The performance of these materials is closely related to their microstructures and, for this reason, to the ways they have been processed. The first step in obtaining high-performance ceramics with a homogeneous microstructure and controlled grain size that meet the requirements of industry is to prepare powders with controlled stoichiometry and small particle size. However, even if a small-size powder is used, conventional sintering is often unable to provide dense, very fine-grained ceramics, due to the high temperatures still required for densification, and the fact that the lowest grain size achievable by classical techniques remains about 0.5 μm or even higher, depending on the system. To solve this problem, the mass transport during the sintering step must be enhanced, since the temperature and time needed for consolidation must be reduced in order to achieve smaller grain sizes. Among the methods reported for activation of the mass transport during the sintering process, the application of an electrical current through the sample during heating represents a promising technique for rapid densification of ceramics at relatively low temperatures. The most novel and increasingly used method is spark plasma sintering, which has clear advantages over conventional sintering methods, making it possible to sinter nanometric powders to near full densification with little grain growth. This has become increasingly important recently, with the miniaturization of electronic devices and the need to investigate size effects on the properties in the sub-micrometer range and approaching the nanometer scale (~100 nm).

In many material applications there is a need for dense materials, often being very close to their theoretical density. Unfortunately, taking account the fragility and refractory properties of ceramic materials and several difficulties inherent in the sintering process, the compaction without any additives becomes a real challenge from both practical and theoretical aspects.

The final electromechanical properties of piezoelectric ceramic components greatly depend upon the history of the ceramic. Each step in the preparation of the material has to be carefully monitored and controlled to obtain the best product. The primary steps of the preparation of the ceramic material are synthesis of the precursor, fabrication of green bodies and, last but not least, sintering of the pellet to achieve proper densification. This third step, which follows powder preparation, consists of thermal treatment with the aim of strengthening the desired piece. It occurs via bonding of the compact grains without melting. Such ''welding'' may be followed

[*] *Dr. A. Castro, Dr. T. Hungría*
Instituto de Ciencia de Materiales de Madrid, CSIC
Cantoblanco, 28049 Madrid, (Spain)
E-mail: thungria@icmm.csic.es
Dr. J. Galy
Centre d'Élaboration de Matériaux et d'Études Structurales/ CNRS 29 rue Jeanne Marvig, B.P. 4347, 31055 Toulouse Cedex 4, (France)

[**] *The Ministerio de Ciencia e Innovación of Spain (through the MAT2007-61884 project) and the Centre National de la Recherche Scientifique (France) are gratefully acknowledged for their financial support. Dr. T. Hungria is indebted to the CSIC (MICINN) of Spain for the ''Junta de Ampliación de Estudios'' contract JAEDOC082.*

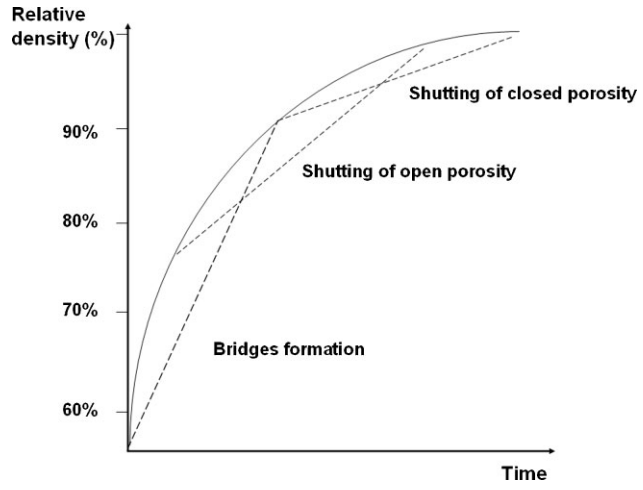

Fig. 1. The three steps of sintering.[1]

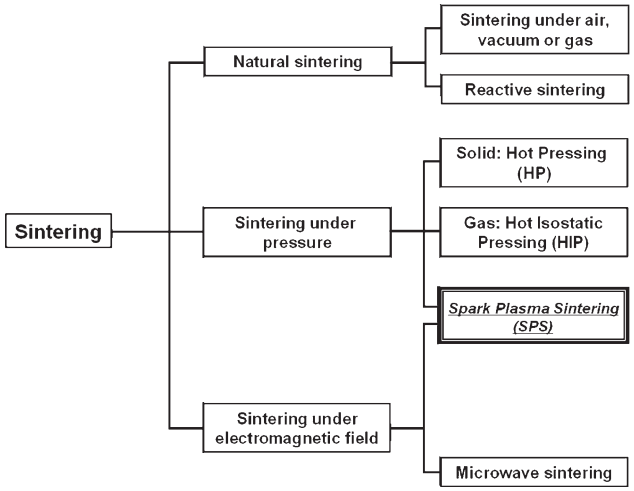

Fig. 2. Different techniques for material sintering.

by a sintering – i.e., porosity reduction – depending on the application of the elaborated product.

In solid-phase sintering, the temperature of the thermal treatment is slightly above two-thirds of the melting point. Sintering is subject of many influences: powder characteristics (morphology, dimension of the grains, purity, etc.), treatment (temperature, pressure, holding time) and atmosphere [vacuum, reducing, oxidizing or inert (Ar, N_2)]. The sintering process of the solid sample is considered to be thermodynamically irreversible. It is expressed by a lessening of the surface energy (free surface of the grains, then surfaces of the open and closed pores). Three steps are defined during the sintering (Fig. 1):[1]

– Formation of a zone of connection between grains, called the bridge or neck of matter. This phenomenon is activated by diffusion mechanisms, evaporation-condensation, plastic deformation, etc., and ends when the bridges have been raised by close to 50% of the grain radii. This step is accompanied by an increase of ~15% of the density.
– Elimination of the residual cavities or pores, the size of which is directly related to the surface energy. Being interconnected, they form a continuous porosity, which diminishes and drives to a compactness of around 90%. Some cavities being instable will lead to some isolated pores.
– The final step corresponds to almost full disappearance of the porosity, giving a fully dense material. Note that the grains tend to grow in this last step.

High-performance materials with high density and uniform microstructure can only be achieved if both composition and grain growth can be controlled. Conventional sintering requires high temperatures and long times for densification; the lowest grain size achievable by this technique remains about 0.5 μm. In addition, for ceramics containing volatile elements (for example alkalines), an exhaustive control of the processing is required in order to maintain compositional homogeneity, because the high temperature and long sintering times cause volatilization of these elements. Hence, alternative sintering methods need to be investigated that enhance mass transport and make it possible to lower both the temperature and the time of consolidation and, thus, to control grain growth.

The objective of these investigations was to enhance mass transport either to make possible the sintering of extremely refractory materials, or to lower the temperature of consolidation. Figure 2 illustrates the different developed techniques. Of these, apart from natural sintering, those based on the application of pressure during the sintering process – for example, hot pressing (HP) and hot isostatic pressing (HIP) – are the most commonly used, allowing dense ceramics to be obtained at lower temperatures whilst inhibiting grain growth. Another means of activating the sintering process involves the use of an electromagnetic field as, for example, in microwave sintering and the spark plasma sintering (SPS), in which pressure is applied simultaneously.

2. The Spark Plasma Sintering Technique

Although the widespread use of an electrical current to activate the sintering process is recent, generated by the availability of commercially built devices, its origin is much older.[2] Early patents describe methods in which an electric discharge is utilized to aid the sintering of powders[3,4] and to obtain synthetic diamonds.[5–8] The use of a current to aid in the processing of different materials has been further developed over the past few decades. Examples of the new generation commercial units include: plasma assisted sintering (PAS); pulsed electric current sintering, (PECS); electroconsolidation, also known as electric pulse assisted consolidation (EPAC); and, perhaps most commonly used, spark plasma sintering (SPS). SPS combines simultaneously the application of pressure and electric current directly on the sample. Joule heating provides high heating rates, allowing dense ceramics to be obtained under uniform heating at

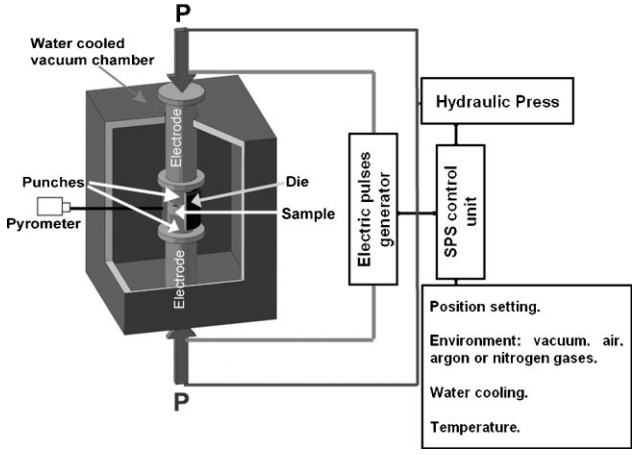

Fig. 3. Schematic drawing of an SPS machine.

relatively low temperatures and in short processing times (typically a few minutes).[9]

The operation of a SPS unit is shown schematically in Figure 3. It consists of a uniaxial pressure device, in which the water-cooled punches also serve as electrodes, a reaction chamber that can be evacuated, a pulsed direct current (dc) generator and pressure-, position- and temperature-regulating systems. In an SPS experiment, a weighed amount of powder is introduced in a die. The die may be built up with various materials, such as carbon, WC, refractory alloys, etc.

The major interest in this process, when the sintering parameters have been mastered, is linked to the extreme rapidity of the thermal treatment. Thus, the consolidation time is greatly decreased from hours, in the case of the conventional sintering, to few minutes for the SPS process. Moreover, the sintering temperature can be diminished by a few hundred degrees compared to conventional sintering (Fig. 4).[10] In short, SPS constitutes an innovative technique in the field of materials sintering and three distinguishing factors contribute

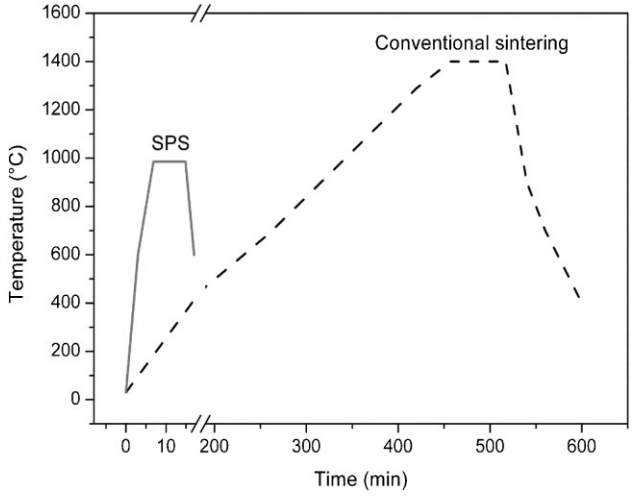

Fig. 4. Comparison of sintering profiles of $BaTiO_3$ ceramics obtained by conventional sintering and by SPS.[10]

to its enhanced densification compared to conventional sintering processes: i) dc current influence, ii) high heating rates, and, iii) the simultaneous application of pressure.

2.1. The Influence of DC Current

The main difference between SPS and other sintering methods is that both die and powder are directly heated by the Joule effect of the dc current. Such techniques make it possible to raise the temperature to 2 000 °C at heating rates of up to 1000 °C min^{-1} or even higher. The role of the current and the sintering mechanism are still subject of many debates between plasma formation[11–16] and electro-migration supporters;[17–19] proof of either of these two phenomena is difficult to find. The plasma problem is complex. Makino has shown that only a very small part of the current (roughly 100 mA) crosses through the Al_2O_3 sample, while some 1 000 A are injected by the machine.[20] In a similar study, Tomino et al. concluded that no current passes trough the sample and eliminated the presence of a discharge in a dense insulator.[21] According to Munir et al., the existence of such plasma or a discharge should be evaluated with different hypotheses, including the applied pressure and the development of the sintering, these two parameters being linked with the formation of large contact surfaces between particles.[2] In the case of conductive powders, there is a good probability of getting discharges between the particles at the beginning of the sintering; therefore, as the sintering progresses, the probability of this occurring decreases.

In spite of the high current, 2 000 A, the current density in a sample of conductive powder 20 mm in diameter should be around 400 A cm^{-2}, a level too low to explain the observed mass transport enhancement. It has, then, been proposed that, due to the extremely small interfacial contact between particles, very high local current densities are present. It is worth noting that for each experiment all the parameters – temperature, pressure, heating rate, holding time, etc. – will be extremely dependent on the nature of the sample and the size of its particles.[22]

The influence of current direction has been tested via solid-state reactivity.[23] Two samples – of Mo/Si and Si/Mo – were reacted at 1 170 °C for 30 min. The micrographs given in Figure 5 show a uniform product layer formation of $MoSi_2$, with the layer thickness being equal at both interfaces. A similar result, i.e., no influence of dc current direction, has been demonstrated on a $V_2O_5/Cu/V_2O_5$ sample with formation of equivalent layer thicknesses of $Cu_xV_2O_5$ phase separated by a metallic Cu phase.[24]

The effect of pulse sequence has also been tested. In an experiment corresponding to Mo/Si syntheses, the pulse pattern being changed from 8:2 to 2:8 did not show any discernible effect on the rate of growth of the $MoSi_2$ layer. Studying this pulse effect on Al_2O_3 sintering, Shen et al.[11] performed experiments at 1 200 and 1 300 °C under a pressure of 50 MPa, with pulse on/off ratios of 10:9, 3:1 and 36:2; the samples were fully dense after a holding time of 3 minutes at

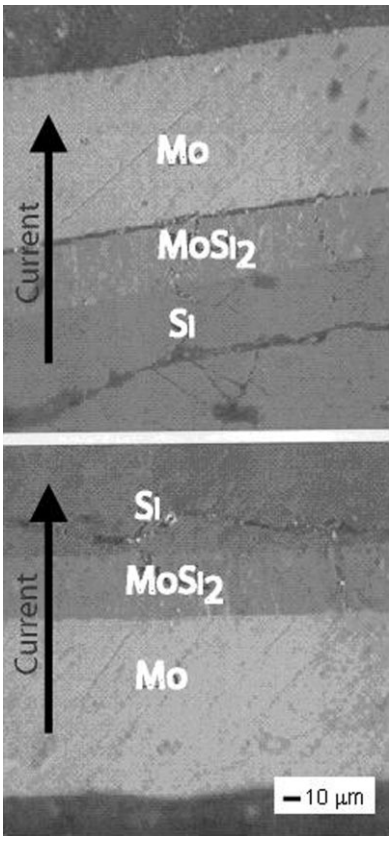

Fig. 5. Micrographs of Si/Mo and Mo/Si samples reacted at 1 170 °C for 30 min with 12:2 (on/off) pulses, note similar $MoSi_2$ interfaces in both cases.[23]

these temperatures and the properties of the ceramics independent of the pulse sequence (Table 1).

Compared to hot pressing, numerous studies have provided clearly evidence that the densification of samples is greatly enhanced in the SPS process. Tokita has shown that, during sintering, matter necks appear between the grains, such a phenomenon being attributed to the presence of plasma between them.[15] Even if the presence of plasma can be debated, it is widely accepted that electric discharges occur at the microscopic level. Another important point has been settled: the influence of pulsing. It has been demonstrated that application of pulsed rather than constant dc current is directly related to the enhancement of the densification of Al_2O_3. The proposed hypothesis to account for this phenomenon is that the discharge of charges accumulated at the critical surface of the particle ionizes the corresponding volume, forming a plasma, which generates a drastic increase in the surface temperature of the particle.

2.2. The Effect of High Heating Rates

The rapid sintering of SPS allows the low-temperature regime, in which the non-densifying mechanism (surface diffusion) is active, to be skipped, proceeding directly to the regime in which the densifying mechanisms (grain boundary and volume diffusion) are predominant.[25] Thus, the grain size decreases as the heating rate is increased.[11] Moreover, densification takes place in very short processing times, which further limits grain growth during the final sintering conditions; SPS provides a unique mechanism to separate grain growth from densification.

By way of example, Shen et al. tested heating rates ranging from 50 to 600 °C min^{-1} in order to obtain fully dense Al_2O_3 ceramics.[11] With heating rates $\leq$350 °C min^{-1}, fully dense samples were obtained, but faster rates yielded porous ceramics. Similar conclusions have been also reported by Zhou et al. on the same powders[26] and a similar behavior was observed during the sintering step of nanosized stabilized ZrO_2.[27,28]

2.3. Simultaneous Application of Pressure

It is generally accepted that the application of mechanical pressure promotes the removal of pores and enhances diffusion. The use of mechanical pressure during the sintering step also increases the density of the green body and, thus, decreases the distance over which mass transfer must occur. Moreover, the extent and rate of particle rearrangement are increased, while the agglomerates are destroyed. From studies carried out in Al_2O_3 and ZrO_2,[11,27,29] it is possible to conclude that the use of mechanical pressure involves a lowering of the sintering temperature and a limitation of the grain growth. These effects can be clearly observed in Figure 6, corresponding to the processing of ZrO_2 by SPS.

The possibility of separately programming the pressure and temperature during the SPS process allows both parameters to be combined in different ways. For example, Guillard et al. investigated the processing of SiC ceramics by two kinds of experiment, keeping the same temperature programme (Fig. 7):[30]

– P-Sw: the maximum pressure was applied only when the maximum temperature (between 1 750 and 1 850 °C) was reached.

Table 1. Influence of pulse sequence on densification and mechanical properties of Al_2O_3.[11]

T_F [°C]	Pulse sequence	Relative density [%]	Grain size [μm]	H_V [GPa]	K_{IcO}
1 200	10:9	99.7	1.0	21.8	3.8
1 200	3:1	99.4	1.1	21.5	3.6
1 200	36:2	99.6	1.4	20.3	3.6
1 300	10:9	100	4.9	18.8	4.2
1 300	3:1	100	4.2	18.0	4.0
1 300	36:2	100	3.3	19.9	3.9

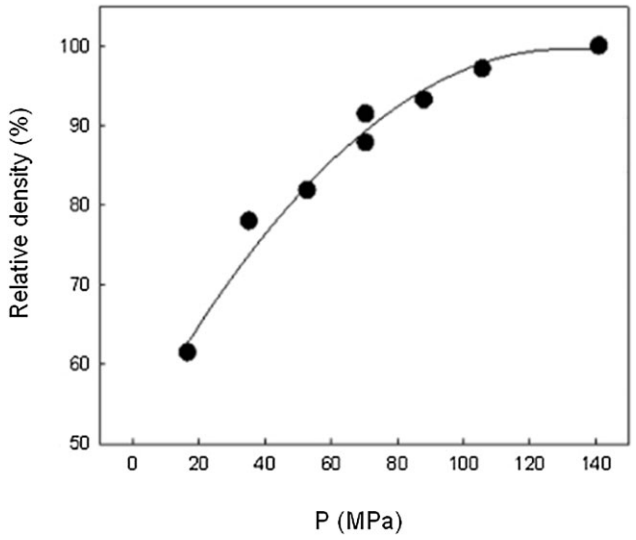

Fig. 6. Effect of the pressure in the densification of ZrO_2 by SPS technique at 1 200 °C and 5 min of holding time.[27]

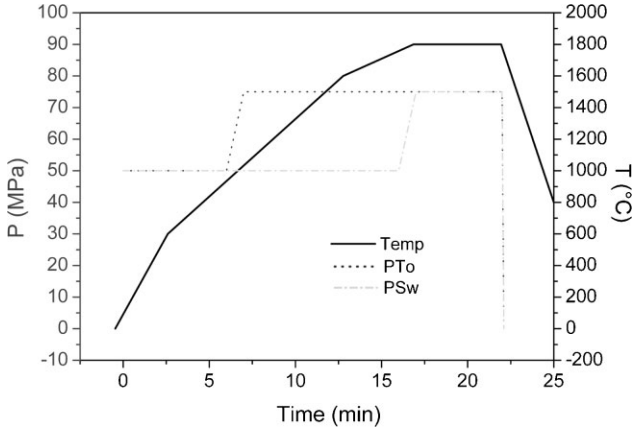

Fig. 7. Temperature rates and temperatures of pressure application in the two protocols Sw and To.[30]

– P-To: the maximum pressure was applied when the temperature was 1 000 °C.

In both cases, the beginning of sintering of the submicrometric SiC powder started at around 1 600 °C and was roughly complete after a few minutes, when the maximum temperature was reached; a longer holding time only favors grain growth. The relative densities of the pellets rose to around 92% for the P-Sw treatment, while for P-To only 80% was obtained. The microstructures of these materials are shown in Figure 8 for the different sintering conditions, which are summarized in Table 2.

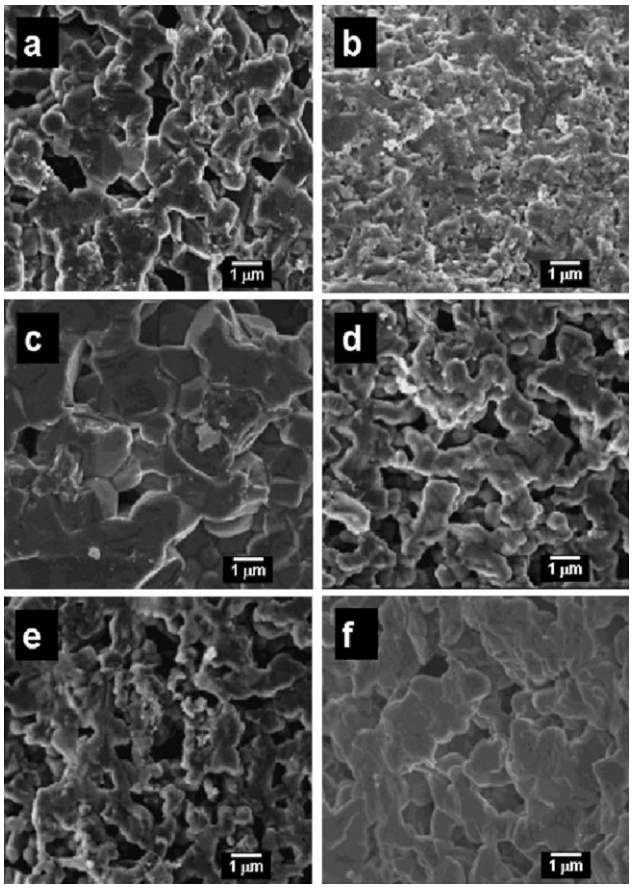

Fig. 8. SEM fracture micrographs of Sw (a,b,c) and To (d,e,f) pellets.[30]

The lower density obtained after the P-To process could be due to the removal of close porosity not being possible with increasing temperature, because the maximum pressure had been applied at 1 000 °C.

2.4. Applications of SPS

SPS is a very powerful technique not only to densify ceramics, but also to prepare many kinds of material. From all the examples found in the literature, three main applications of this sintering technique can be discerned:

Table 2. Data for the SEM micrographs shown in Figure 8.

Protocol	Pellet	T [°C]	Holding time [min]	Experimental density [g cm^{-3}]	Relative density [%]	Grain size [μm]
Sw	a	1 780	1	2.51	78	0.5
Sw	b	1 780	10	2.82	88	0.8
Sw	c	1 850	5	2.95	92	2.0
To	d	1 780	1	2.33	72	0.5
To	e	1 780	10	2.36	73	1.0
To	f	1 850	5	2.41	75	2.5

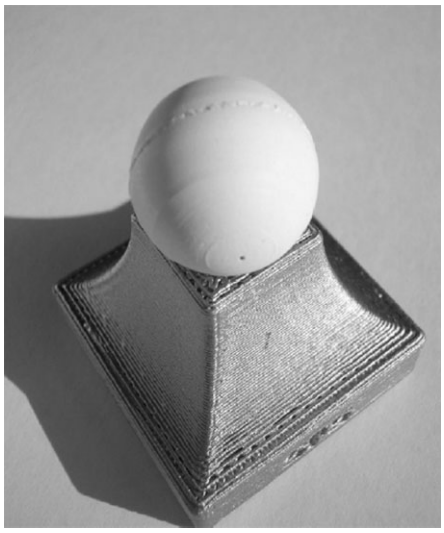

Fig. 9. Al_2O_3 sphere obtained in one single step by SPS.[63]

2.4.1 Compaction of Ceramics

SPS has been demonstrated to enable the consolidation of ceramics materials within minutes and the ability to obtain fully dense samples at comparatively low sintering temperatures, typically a few hundred degrees lower than in normal hot pressing. The most commonly compacted materials by this technique are: carbides, for example, SiC, Ti_3SiC_2, WC and ZrC;[30–38] nitrides, for example Si_3N and AlN;[39–41] oxides, for example, ZrO_2,[27,28,42] Al_2O_3[9,11,43] and several perovskites;[10,44–49] phosphates, for example, Nasicon[50] and Hydroxyapatite;[51,52] metals;[53-56] intermetallics;[57] and, borides.[58,59] The use of rapid sintering appear to be essential for the fabrication of nanocrystalline ceramics[46,49] and to get special microstructures.[60]

Using SPS as a forming tool is a relatively new idea.[61,62] The near-net-shape forming method means that a minor amount of machining and polishing is needed. Obviously, the overall cost for making a shaped part by using this method is drastically decreased. The fast heating and forming process also ensure minimized grain growth and, therefore, the unique properties of nano-scale materials may be obtained. Figure 9 shows a picture of an Al_2O_3 sphere obtained in a single step from commercial Al_2O_3 powder by SPS at 1250 °C and 75 MPa.[63]

2.4.2 Preparation of Composites

In situ processing of composites is, compared to conventional processing, advantageous for obtaining materials with a finer and more homogeneous microstructure, high chemical and thermodynamical stabilities at a higher temperature, and better mechanical properties.[64] SPS can be used to process a wide range of materials because of its short sintering time, which avoids reactions between the material components, as can be observed in the example of the processing of Al_2O_3/Cr_2O_3 (Fig. 10). In this figure it is possible to observe not only the appearance of the interface (Fig. 10a), but also the analysis of a cross-section of the polished pellet performed with a microprobe (EPA) Cameca SX 50 (Fig. 10b).[65] Some other interesting systems are described in the literature, for example, the pseudo-binary system Al_2O_3–$Y_3Al_5O_{12}$,[66] hydroxyapatite–Ag composites avoiding metal volatilization,[67] short carbon-fiber reinforced SiC matrix composites,[68] and Al_2O_3/single-wall carbon nanotubes (SWNT).[69]

2.4.3 SPS in situ Reaction Sintering

Some recent studies show the possibility of using the SPS technique not only to create a fully dense material, but also to synthesize the constituent phases of the ceramics. For example, it is possible to obtain TiN/Al_2O_3 nanocomposites using Ti, AlN and TiO_2 commercial powders as starting materials. This novel fabrication process for a TiN/Al_2O_3 nanocomposite basically involves molecular-level mixing of the TiN and Al_2O_3 during a reaction process, instead of conventional powder mixing. The as-prepared TiN/Al_2O_3 nanocomposite has a finer microstructure with a grain size below 400 nm, and exhibits better mechanical properties.[70] Similar results were observed for a mixture of Ti, C and Si powders to obtain Ti_3SiC_2–SiC composites.[71] In the case of the refractory materials, as for example HfB_2, the simultaneous synthesis and sintering produced dense ceramics (with 98% of the theoretical density) at lower pressure and temperature.[72]

In order to explore the possibility of using SPS as a technique to can carry out a new sort of solid-state chemistry, the behaviour of the system M/V_2O_5 (M = Ag, Cu, Zn) during the SPS process has been investigated. The formation of different $M_xV_2O_5$ phases has been observed in a few minutes, even without a holding time at the final sintering conditions (Fig. 11).[24,73] An interesting route is now open to

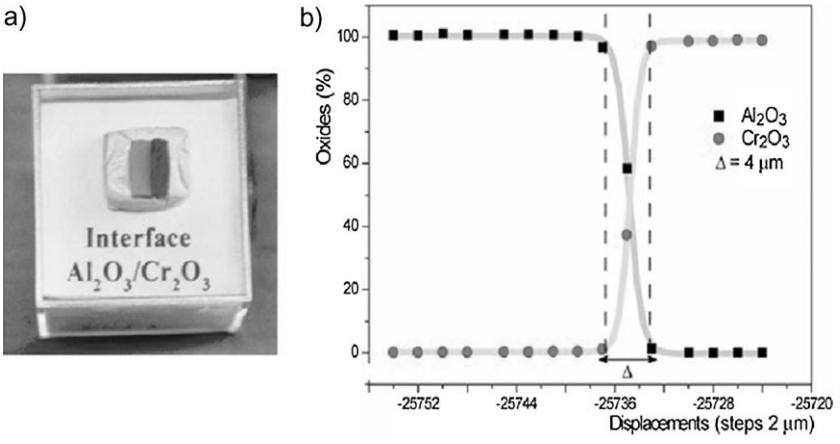

Fig. 10. a) Al_2O_3/Cr_2O_3 interface prepared by SPS (1250 °C, 75 MPa, 3 min), and, b) EPA of the cross-section of the pellet.

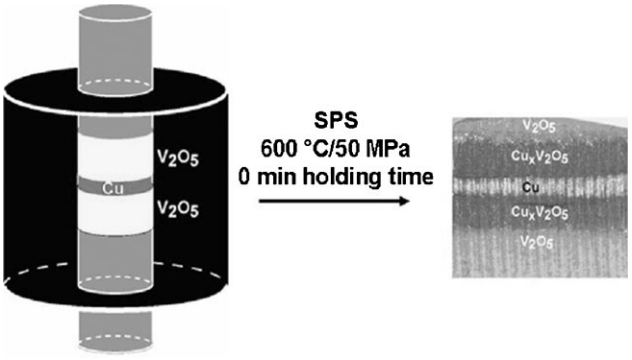

Fig. 11. Behavior of the Cu/V_2O_5 system during the SPS experiment.[24]

use SPS to develop new solid-state chemistry under the simultaneous influence of temperature, pressure and an electrical current.

In summary, a huge quantity of experiments can be carried out by this powerful technique with the aim of forming high-temperature and/or high-pressure stable phases, as well as the evident possibility of obtaining fully-dense, fine-grained or even nanostructured ceramics.

In the next section of this work, the application of the SPS technique to the preparation and improvement of piezo-ferroelectric materials is reviewed.

3. SPS Applied to the Preparation of Piezo-Ferroelectric Ceramic Materials

3.1. Generalities on the Processing of Piezo-Ferroelectric Oxides

It is well known that the properties of a ceramic material are greatly influenced by its microstructural characteristics, including: porosity, grain size, morphology, defects, etc. Hence, the sintering step to process ceramic materials has very much importance with respect to the final response of the material. As mentioned above, ceramic forming processes may be classified as classical – such as die pressing, cold isostatic pressing, slip casting and extrusion – or as new and emerging – for example, injection moulding and tape casting. Some traditional methods have been improved to meet particular property requirements; these include hot pressing, hot-isostatic pressing, hot forging and pressure casting.

Most of the above-mentioned methods have been applied to the sintering of piezoelectric materials, depending on the particular characteristics of each compound, like morphology of the starting powders, chemical compositions with possible volatilization of components (Na, Pb, Bi, . . .), trend toward exaggerated grain growth, etc. By way of illustration, abnormal grain growth along with crack generation and pore formation is frequently encountered in tungsten–bronze ferroelectric ceramics prepared by conventional sintering methods, which appreciably deteriorates their physical properties.[74,75] Several strategies have been used to solve such problems, including hot pressing (HP),[76,77] hot isostatic pressing (HIP),[77] dual-stage sintering[75] and the addition of sintering aids.[78]

Concerning sodium and potassium niobates, until a few years ago there have been only a few reports about the piezoelectricity of $NaNbO_3$, $KNbO_3$ and $NaNbO_3$–$KNbO_3$ ceramics, probably because of their poor sinterability and the high volatility of the sodium and potassium components during the sintering process. However, good electrical properties can be found on dense $Na_{0.5}K_{0.5}NbO_3$ ceramics prepared by hot-pressing methods.[79,80]

The materials derived from lead titanate are the most studied from the point of view of their applications in piezoelectric devices, so that the fabrication of high-quality ceramics has become one important challenge. By way of examples, it was observed that the dielectric constant in $PbMg_{1/3}Nb_{2/3}O_3$–$PbTiO_3$ materials is grain-size dependent, and increases with increasing grain size.[81–83] The relative role of extrinsic mechanisms, like domain wall motion in piezoelectric properties, was deduced to be strongly influenced by grain size.[84] For these reasons, attempts have been made to prepare ceramics with controlled grain growth and high relative density by applying different techniques,[85–88] including conventional pressure-less sintering, microwave sintering, or hot-isostatic pressing. Analogously, the application of hot pressing and atmosphere-controlled sintering has been reported for the fabrication of transparent PLZT (lanthanum-modified lead zirconate titanate) ceramics.[89–91] However, long sintering periods are needed for these procedures, giving rise to extremely large grains that are detrimental to the mechanical strength of the ceramics.[92]

Finally, it is well established that the properties of $BaTiO_3$-based ceramic materials strongly depend on their microstructure and grain size.[93] However, high density $BaTiO_3$ ceramics with nanometer grain size (<100 nm) are difficult to obtain, because of grain growth taking place during the final stage of densification processes, which is always at high temperature.[94] In this way, Oonishi et al.[95] attained dense $BaTiO_3$ ceramics (above 98% relative density), but with submicrometer grains (0.2–0.6 μm), by hot-isostatic pressing.

In conclusion, improved performance, high permittivity miniaturized devices can be achieved by controlling the ceramic microstructure, such as grain size and homogeneity, which depends on the properties of the starting powder and the sintering method. One final objective must be to maintain a nanosized microstructure after sintering, in order to obtain improved properties. Such challenges could be accomplished by using the SPS technique, which enables a compact powder to be sintered under uniform heating, to high density at relatively lower temperatures and in much shorter sintering periods, typically of a few minutes, compared with other sintering methods.

3.2. Insights on Processing by Spark Plasma Sintering

The SPS method has been used to obtain a large variety of piezoelectric ceramics, belonging to different structural types

and with diverse chemical compositions. Here, the main results reported are reviewed, ordered according to the structural types of the starting oxides: 3-D perovskites, lead-free ($BaTiO_3$-based and $ANbO_3$-based materials) and high-sensitivity piezoelectrics ($PbTiO_3$-based ceramics); BLSFs or layered perovskites (Aurivillius-type phases), as high-temperature piezoelectrics; and, relaxor tungsten bronzes.

3.2.1. $BaTiO_3$-Based Lead-Free Materials

This system is one of the most studied using SPS, with the first work, reported in 1999 by Takeuchi et al.,[44,96] showing the processing of dense $BaTiO_3$ ceramics (~95–97% densification). The starting powders are synthesized by different methods, either hydrothermal, hydrolysis or solid-state route (SSR), allowing sub-micrometer grain sized materials (typically 0.1 to 0.6 μm) to be formed, with grain size similar to that of the starting powder. It has been demonstrated that the SPS process is effective for stabilizing the metastable cubic phase and also in reducing the influence of intergranular (grain boundary) effects on the permittivity and dc resistance, both characteristics of $BaTiO_3$ ceramics. Fixed-frequency, 1 kHz, permittivity data for SPS and SSR pellets over the temperature range 25–300 °C are shown in Figure 12. Although all data show a maximum at the ferroelectric Curie temperature of approximately 120 °C, SPS samples show higher permittivity values, particularly below the Curie temperature.[44]

Subsequent studies by the same research group,[97,98] have also shown the influence of the synthesis method of perovskite powder on the properties of the final materials; for example, ceramics prepared from $BaTiO_3$ powder processed by a sol-gel method exhibit high room temperature permittivity values compared to conventional sintered ones. This fact is attributed to electrical inhomogeneities within pellets: a resistive surface layer covers the inner pellet core that consists of oxygen-deficient $BaTiO_3$. The reduced pellet core is characteristic of SPS ceramics, formed from powders that contain small amounts of residual organic matter.[97]

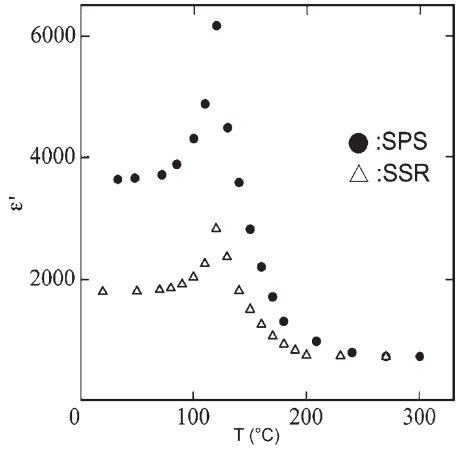

Fig. 12. Temperature dependence of the permittivity at 1 kHz for SPS and SSR $BaTiO_3$ pellets.[44]

Several articles have been devoted to reporting the influence of the grain sizes of $BaTiO_3$ ceramics on their properties, down to the nanometer scale. SPS technology is particularly suitable for control of the grain size of the materials, of course depending on the average particle size of the precursor powders. The synthesis methods chosen to obtain nanosized powders are: sol-gel,[99–100] coprecipitation,[94,99,101–102] self-propagating high-temperature synthesis[103] and hydrothermal processing.[104–105]

The works of Li et al.[94,99] analyze the influence of both synthesis method and SPS conditions, such as heating rate, holding time and sintering temperature, etc., on the densification, grain size, grain shape and dielectric properties of the obtained material. It is easily concluded that the dielectric constant at the transition temperature decreases and T_c shifts to lower temperature with decreased grain size. This can be explained by the decreased tetragonal polymorph content and the internal stress remaining in the ceramics with reduced grain size. Other authors[100] also report the preparation of nanostructured $BaTiO_3$ ceramics, where a small proportion of cubic phase can be found, in contrast with conventional-sintered ceramic, which is a single tetragonal phase. This fact is correlated with the existence of diffuse phase transition phenomenon on fine-grained SPS ceramics.

Buscaglia et al. carried out a thorough study, by AFM piezo-response and micro-Raman spectroscopy, of nanostructured ceramics prepared using SPS.[101,102] They obtained $BaTiO_3$ ceramics with an average grain size of about 50 nm, showing a broad phase transition with a maximum of permittivity at 120 °C. The maximum relative dielectric constant had a value remarkably lower than those reported for coarse ceramics. Local switching of ferroelectric domains was probed by piezoresponse force microscopy. Figure 13 shows the sample's topography (Fig. 13a) and hysteresis loops from two different regions (Fig. 13b). Regions with zero piezo-response and non-hysteretic behavior were also found. The different types of piezo-response observed in the nanocrystalline ceramics can be related to a distribution of tetragonality (and polarization), over the volume of the ceramic, induced by structural inhomogeneities of the material. The results indicate that the possible critical grain size for disappearance of ferroelectricity in $BaTiO_3$ ceramics is below 50 nm. They were also able to prepare nanosized powders with grain sizes in the range 20–30 nm by the self-propagating high-temperature synthesis method and subsequent mechanical milling.[103] The ceramics obtained by SPS from those powders exhibited relative densities in the range 66–99%. The Curie temperature was again shifted to lower temperatures (108 °C) and the relative dielectric constant significantly depressed by the dilution effect, due to the presence of a non-ferroelectric low permittivity grain boundary layer.

Analogous work recently performed by Deng et al.[104,106] conflicts with the results just described. They use Raman spectra and X-ray diffraction data, in combination with electron microscopy, to study the evolution of lattice structure

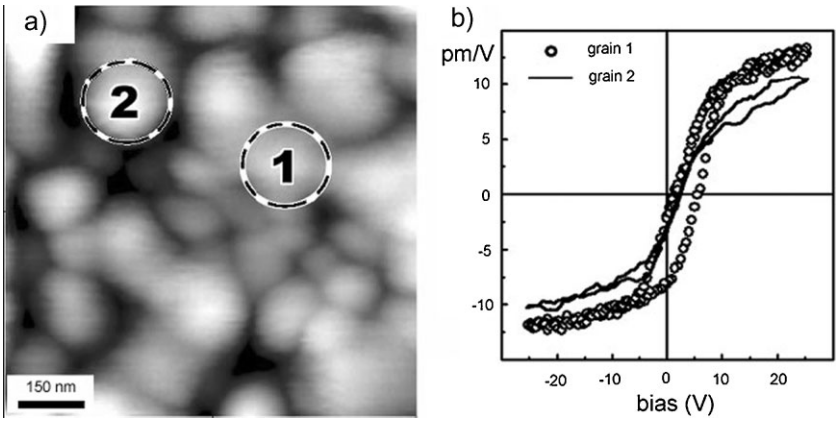

Fig. 13. a) AFM-topography of the surface of a BT ceramic with average grain size of 50 nm, and, b) piezoelectric hysteresis loops recorded from the regions marked as '1' and '2' in a).[101]

and phase transformation behavior with grain growth, from nano- to micrometer-scale, for $BaTiO_3$ ceramics. They also investigate their polarization-reversal characteristics and the local ferroelectric switching behavior, by scanning force microscopy in piezoresponse mode, providing experimental evidence that, if a critical grain size exists for ferroelectricity, it is less than 20 nm.

On the other hand, $BaZr_{1-x}Ti_xO_3$ (BZT) materials exhibit ferroelectric-relaxor characteristics. More specifically, a mild temperature-dependence of the dielectric constant has been observed of $BaZr_{0.2}Ti_{0.8}O_3$ thin films with grain size < 100 nm. In order to prepare fine-grained and dense BZT ceramics, Maiwa[107] selected the SPS method. This method also enables ceramics of this family to be obtained with high densities and small grains, which exhibit less hysteretic field-induced strain loops than those prepared by classical methods.

SPS has also been applied to obtain dense ceramics belonging to the solid solution $Ba_{1-x}Sr_xTiO_3$.[10,108–111] The works of Hungría et al.[10] and Nygren et al.[108–110] should be highlighted. The first authors reported the mechanosynthesis of nanocrystalline powders with compositions $Ba_{1-x}Sr_xTiO_3$ ($x = 0$, 0.25, 0.5, 0.75 and 1), which form a solid solution over the whole range of compositions. This work was the first to report the combination of mechanosynthesis and SPS to obtain electroceramics; the combination was used to process ceramics of the Ba–Sr–Ti–O system, with very high density and homogeneous microstructure, at a temperature 300–400 °C lower than that for conventional sintering of $Ba_{1-x}Sr_xTiO_3$ phases, obtained by solid-state reaction. This approach allows grain growth to be controlled and opens the possibility of processing fully dense nanostructured ceramics. Dielectric permittivity as a function of temperature was characterized for a series of samples, across the solid solution, and it was confirmed that dense, fine-grained ceramics can be processed by this novel approach for all compositions investigated (Fig. 14).

Nygren et al. focused their studies on same system, but at composition $x = 0.4$.[110] They compared the behavior of the commercial nanometric (60–80 nm) $Ba_{0.6}Sr_{0.4}TiO_3$ (BST64) powder with a mixture of the commercial nanometric (60–80 nm) $BaTiO_3$ and $SrTiO_3$, with the same Ba/Sr ratio, produced by ball milling (MBST64). They determined the "kinetic window" of these SPS experiments – defined as the temperature interval within which the densification step can be separated from the grain growth one – enabling the processing of dense nanostructured ceramics. The width of this window is 125 °C for MBST 64, while it is almost zero for the commercial BST64 nanopowder. The densification of the former powder is accompanied by a solid-state reaction and the main part of this reaction takes place within the fully densified compact, suggesting that the grain growth is retarded in the reactive sintering. It appears that it is much more feasible to master the sintering kinetics by the SPS technique than by HP, HIP or any other conventional sintering process, as in these processes it is difficult to avoid the comprehensive grain growth, especially during the final stage of sintering.

Finally, Takeuchi and Kageyama also used the SPS method to prepare composite dielectric ceramics of $BaTiO_3$/$SrTiO_3$.[112] The short sintering time (~3 min) needed by this technique is advantageous in suppressing the formation of a complete solid solution $(Ba,Sr)TiO_3$. It was verified that the actual SPS–$BaTiO_3$/$SrTiO_3$ composites consisted of $BaTiO_3$ and small amounts of $(Ba_{1-x}Sr_x)TiO_3$, with various x values, having different phase transition temperatures. Such multicomponent microstructures would be responsible for a flat temperature dependence of permittivity.

In the same way, other composite or nanocomposite materials, based on $BaTiO_3$, have been prepared. In particular, densified multi-walled carbon nanotube (MWNT)–$BaTiO_3$ composites were successfully fabricated through an SPS method by Huang et al.[113,114] Moreover, piezoelectric fully dense $BaTiO_3$/MgO (pre-sintered)/$BaTiO_3$, $BaTiO_3$/MgO

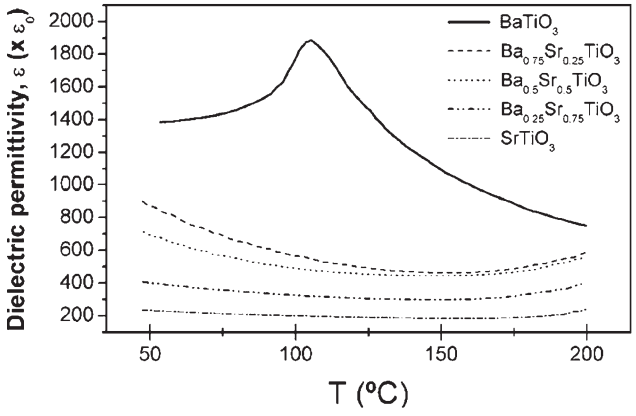

Fig. 14. Temperature dependence of the permittivity of the $Ba_{1-x}Sr_xTiO_3$ ceramics processed from mechanosynthesized precursors by SPS at 1100 °C and 100 MPa for 3 min.[10]

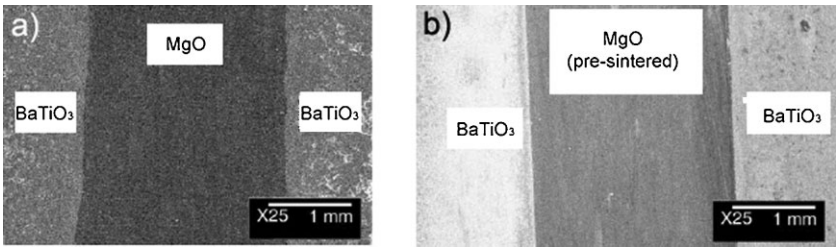

Fig. 15. Micrographs of the cross-sections of: a) $BaTiO_3$/MgO/$BaTiO_3$, and, b) $BaTiO_3$/MgO(pre-sintered)/$BaTiO_3$ laminates processed by SPS.[115]

with 10 vol.-% $BaTiO_3$/$BaTiO_3$ laminate composites, have been successfully fabricated as a smart material by an SPS process (Fig. 15). From EDS analysis, no reaction between $BaTiO_3$ and MgO layers was observed along the interface.[115] SPS has also been suitable to consolidate almost fully dense $BaTiO_3$/Al_2O_3 nanocomposites.[116]

To finish this section, the usefulness of SPS can also be seen for the fabrication of dense bulk dielectric materials, with a locally graded (core-shell) structure. A very exciting example is the sintering of $BaTiO_3$ particles, coated with two different perovskites ($SrTiO_3$, $BaZrO_3$).[117] The synthesis entails growing the shell of $SrTiO_3$ or $BaZrO_3$ directly on the surface of $BaTiO_3$ spherical templates, suspended in aqueous solution by means of a precipitation process. Dense ceramics, with locally graded structure and a limited interdiffusion between core and shell regions, can only be obtained by a careful choice of the sintering conditions and, in the particular case of $BaTiO_3$/$SrTiO_3$, by using the SPS technique (Fig. 16).

3.2.2. Alkaline Niobate Lead-Free Materials

Although alkaline niobate-based piezoceramics exhibit an important combination of electrical and mechanical properties and an environmentally friendly character, the processing of high-quality ceramics remains a challenge. Moreover, for alkaline niobate ceramics, control of the processing is required in order to improve the compositional homogeneity, because high temperature and long sintering times lead to volatilization of the alkaline metal.[118] In most of these systems,

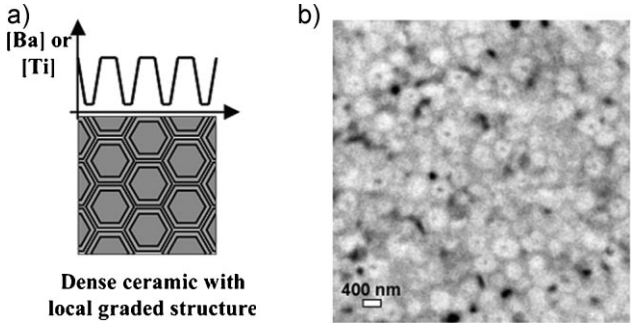

Fig. 16. a) Schematic illustration of the ceramic obtain by sintering of the core-shell particles to a dense ceramic with limited interdiffusion, and, b) backscatter electron image of the polished surface of a $BaTiO_3$@$SrTiO_3$ ceramic (densified by SPS at 1 100 °C for 2 min, overall composition $Ba_{0.66}Sr_{0.34}TiO_3$) revealing a concentric, non-uniform distribution of Sr and Ba.[117]

temperatures as high as 1 200 °C are necessary; however, abnormal grain growth occurs at these temperature ranges (especially in $NaNbO_3$-rich compositions), and incipient microstructure degradation is observed. For these reasons, SPS seems to be one of the most suitable methods to enhance mass transport, lowering both the temperature and time of consolidation.

The first attempts to applied the SPS method to obtain alkaline niobate related ceramics were made by Wang at al. and Wada et al., who both succeeded in processing dense ceramic – $(1-y)(Na_{0.5}K_{0.5})NbO_3$–$yPbTiO_3$ ($y \leq 0.5$) and $NaNbO_3$, respectively – in order to study their electrical responses.[119,120]

One of the more studied solid solutions of this system is $Na_xK_{1-x}NbO_3$, due to the good piezoelectric properties it is expected to have; however, because of its poor sinterability under ambient pressure, research has been devoted to new processing methods. The study by Wang et al.,[121] using the SPS method, clearly showed that ceramics with ~98% densification can be obtained at temperatures of 1 040–1 100 °C ($x = 0.5$, 0.6 and 0.7). The authors also characterized SPS-sintered ceramics, comparing the results to hot-pressed ceramics. They conclude that SPS-sintered $Na_xK_{1-x}NbO_3$ samples possess higher room temperature dielectric constants, higher coercive fields, lower remnant polarizations and lower electromechanical coefficients. All these results seem to be related to the smaller grain sizes, or the consequently larger grain boundary areas. The same system was also studied by Li et al. for x values ranging between 0.2 and 0.8.[122,123] They obtain ceramics with a high degree of densification when SPS was carried out at a temperature as low as 920 °C.

To be precise, the density of the $Na_xK_{1-x}NbO_3$ ceramics decreased with increasing Na content, from a relative value of 99% for the K-rich side to 92% for the Na-rich side, as can be observed in Figure 17.[122] A detailed study of the ferroelectric and piezoelectric properties of the $Na_{0.5}K_{0.5}NbO_3$ ceramic sample (SPS: 920 °C and 99% theoretical density) showed typical ferroelectric and piezoelectric characteristics (Fig. 18). Although the grain size is small, about 200–500 nm, the resultant ceramic shows a considerably high d_{33} of 148 pC N^{-1}.[123]

In addition, the SPS technique has been employed to prepare dense ceramics belonging to more complex systems, for example $(1-x)Na_{0.5}K_{0.5}NbO_3$–$xSrTiO_3$ ceramics.[124–126] In general, the authors establish a detailed phase diagram for the solid solution, in order to determine the composition of the tetragonal–orthorhombic morphotropic phase boundary, which can be found in the vicinity of $x = 0.05$. Around the morphotropic phase boundary, k_p as well as d_{33} show a similar behavior to that in lead-based piezoelectric materials.[124]

Recently, for the sake of comparison, $NaNbO_3$–$SrTiO_3$ ceramics have been processed by conventional sintering and

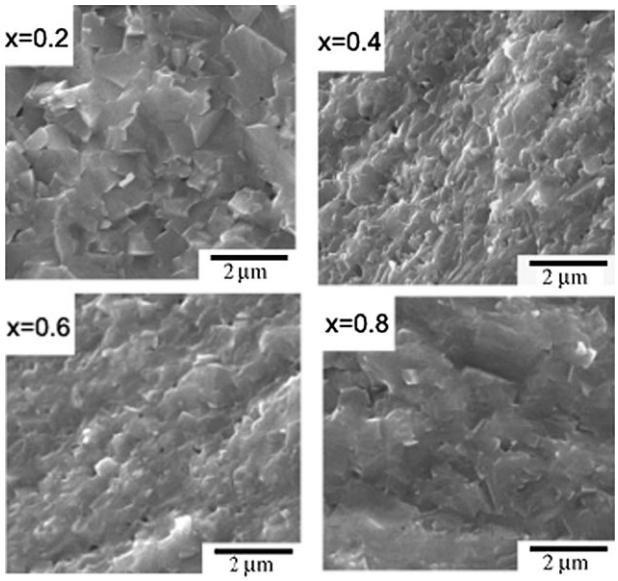

Fig. 17. SEM micrographs of $Na_xK_{1-x}NbO_3$ ceramics with various Na content.[122]

SPS, from the nanocrystalline perovskites obtained by mechanosynthesis. Two significant drawbacks were observed during the sintering of ceramics from very reactive mechanosynthesized precursors by conventional methods:[118] i) the inability to process dense $0.1NaNbO_3$–$0.9SrTiO_3$ ceramics below 1 300 °C, and, ii) abnormal grain growth in the case of the $0.9NaNbO_3$–$0.1SrTiO_3$ composition, which resulted in large square-shaped grains of 50–100 μm and a degraded density. The combination of mechanosynthesis and SPS makes it possible to control grain growth down to the submicrometric scale and to obtain homogeneous microstructures, demonstrating the synergy between these two non-conventional methods (Fig. 19).[48] Dielectric properties have been measured across the main phase transitions in the system for submicrometer-structured ceramic materials processed by SPS, and are comparable with those of ceramics prepared by conventional sintering.

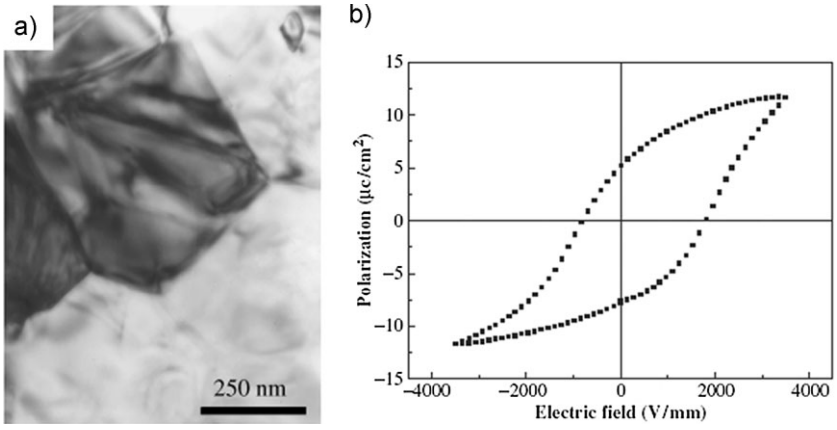

Fig. 18. a) Transmission electron microscopy micrograph of the $Na_{0.5}K_{0.5}NbO_3$ ceramic prepared by SPS, and, b) polarization hysteresis curve of the same ceramic.[123]

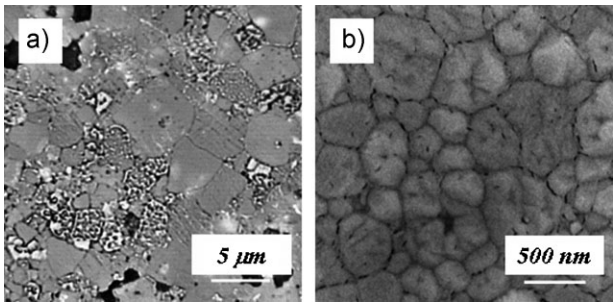

Fig. 19. Micrographs of the polished surfaces of $0.9NaNbO_3$–$0.1SrTiO_3$ ceramics processed by different means: a) conventionally sintered at 1 100 °C for 2 h (optical micrographs), and, b) SPS at 1 100 °C/50 MPa (scanning electron micrographs).[48]

3.2.3. High-Sensitivity Piezoelectrics Chemically Derived from $PbTiO_3$

The first works dealing with the application of SPS to $PbTiO_3$-related materials report results corresponding to the parent compound. It can, therefore, be deduced that the nature of the powdered precursors have a great influence on the results. Kakegawa et al. claim that lead titanate ($PbTiO_3$) is difficult to sinter without additives, even when an SPS technique is applied, if a simple mixture of PbO and TiO_2 is employed as the precursor.[127] This fact is attributed to the mechanical strain that resulted from the phase change from cubic – the stable polymorph at the sintering temperature – to the tetragonal stable phase at room temperature, after the sintering, which allows a decrease in the grain size, rather than and increase of densification, to be reached. In contrast, other authors have succeeded in obtaining dense $PbTiO_3$ ceramics consisting of submicrometer-sized grains (0.1 μm) by using SPS.[47] This difference must be due to the precursor employed, in the latter case, hydrothermally prepared $PbTiO_3$. The powder was densified to about 98% of the theoretical density and the average grain size of the ceramics was ≤1 μm (Fig. 20a), even after sintering at 900–1 100 °C. The measured permittivity for the SPS ceramics showed almost no frequency dependence over the range 10^1–10^6 Hz, their coercive field being greater than that of conventional sintered materials. Moreover, the P–E hysteresis loops (Fig. 20b) show that the SPS process induces a decrease in the measured ferroelectric response of the $PbTiO_3$ ceramics, probably because of the fine-grained microstructures of the SPS pellets; this fact was attributed to their finer microstructure.

On the other hand, studies carried out on $PbZr_{0.3}Ti_{0.7}O_3$ ceramics[128] suggested that SPS, combined with a further heat treatment, could be used to control the compositional distribution of this material, which has pronounced effects on many of its properties.

One of the PT-based systems to which the SPS technique has been widely applied, in order to obtain ceramics with enhanced

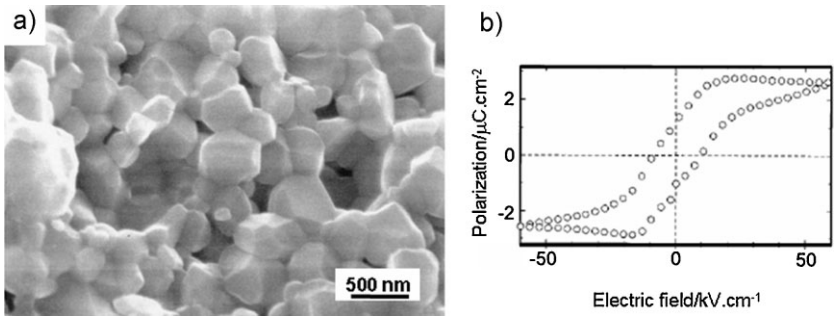

Fig. 20. a) SEM photograph of fracture surfaces of SPS pellets sintered at 1 000 °C for 1 min, and, b) P–E hysteresis loops of the same ceramic.[47]

properties, is the solid solution $Pb(Mg_{1/3}Nb_{2/3})O_3$–$PbTiO_3$.[129–133] The SPS process has also been determined to be very effective for the densification of $0.65Pb(Mg_{1/3}Nb_{2/3})O_3$–$0.35PbTiO_3$ ceramics. This fact is very important because, in this material, the higher the density and the larger the average grain size, the better the dielectric and piezoelectric properties that are obtained. Moreover, the SPS process allows a capillary driven 0.65PMN–0.35PT single crystal to be fabricated, with a high density, by increasing the density of the polycrystalline matrix precursor during heat treatment.[131] Very recently, a deeper study, carried out by Zuo et al.,[132] showed that a strongly frequency dependent and broad diffuse phase transition can be observed for all SPS samples, together with low remnant polarization and strain, and a high coercive field. These exceptional electrical properties of SPS samples are attributed to the fine grain size and the heterogeneity in microstructure and composition.

Similarly, the SPS method has been applied to the obtaining of dense ceramics belonging to the system $xPb(Zn_{1/3}Nb_{2/3})O_3$–$yPbZrO_3$–$(1-x-y)PbTiO_3$. When a mixture of calcined materials, having different compositions of this system, was sintered by SPS, the compositional distribution in the starting mixture was almost maintained and such material exhibited a high pyroelectric coefficient, strongly related to the microstructure, over a wide temperature range.[134,135] Moreover, SPS has been also used as a new method of preparing transparent $xPb(Zn_{1/3}Nb_{2/3})O_3$–$yPbZrO_3$–$(1-x-y)PbTiO_3$ ceramics that could be promising candidates for applications in areas such as electro-optics and pyro-optics.[136]

A result of great importance to be highlighted is the successful use of the combination of mechanosynthesis and SPS for the preparation of nanostructured $0.92PbZn_{1/3}Nb_{2/3}O_3$–$0.08PbTiO_3$ ceramics. This approach allows the PZN–PT perovskite to be stabilized and, at the same time, grain growth to be controlled. In such a way, ceramics with a major perovskite phase were obtained at temperatures of 550–600 °C, with a grain size of ~15–20 nm (Fig. 21).[137] The electric characterization of this material indicates that the relaxor to ferroelectric phase transition does not occur on the nanoscale, and that a relaxor state does exist, instead of the ferroelectric phase. An electrical polarization can be built up and switched with an electric field in the $0.92Pb(Zn_{1/3}Nb_{2/3})O_3$–$0.08PbTiO_3$ nanostructured material.[49]

There have been some other results reported on the application of the SPS method to obtain dense ceramics of lead titanate-based high-sensitivity piezoelectric materials. These works deal with $Pb_{0.97}La_{0.02}(Zr_{0.77}Sn_{0.14}Ti_{0.09})O_3$,[138] $Pb_{0.97}La_{0.02}(Zr_{0.76}Sn_{0.11}Ti_{0.13})O_3$,[139] $Pb_{0.92}La_{0.08}(Zr_{0.65}Ti_{0.35})_{0.98}O_3$,[140] $0.64Pb(Ni_{1/3}Nb_{2/3})O_3$–$0.36PbTiO_3$[141] and even $(1-y)(Na_{0.5}K_{0.5})NbO_3$–$yPbTiO_3$ $(y \leq 0.5)$.[119]

As a general conclusion, the SPS technique allows almost fully dense ceramics to be prepared with largely improved properties; this is mainly attributed to the control of their chemical compositions and microstructures. Obviously, the synthesis method for the powdered precursors and the result morphology of those powders also has a drastic effect on the characteristics of the final ceramic material.[10]

3.2.4. High-Temperature Piezoelectrics Belonging to the Aurivillius-Type Structure

The pioneering work on the consolidation of Aurivillius-type ceramic materials by SPS appeared nine years ago, when Takehashi et al. reported obtaining grain-oriented samples of $Bi_4Ti_3O_{12}$ with a strong anisotropy in their electrical properties.[142] No new reports on SPS-processed ceramics of this oxide, or any other Aurivillius compound, can be found up to 2003, when Wu et al. reported the preparation of $BaNd_2Ti_4O_{12}/Bi_4Ti_3O_{12}/BaNd_2Ti_4O_{12}$ composite-laminated ceramics by the combination of SPS with a subsequent heat treatment.[143] In this work, the authors highlight that SPS combined with heat treatment provides a new approach to prepare laminate ceramics, from compositions having quite different sintering temperatures.

Later, two studies on $n=2$ Aurivillius phases, $SrBi_2Ta_2O_9$ and $BaBi_2Nb_2O_9$, again showed the possibility of fabricating dense and grain-oriented ceramics with enhanced properties.[144–145] Moreover, Li et al. showed the improvement of SPS method to prevent the decomposition of $SrBi_2Ta_2O_9$ ceramics, and then to maintain their ferroelectric properties. In fact, it is well known that at temperatures higher than 1 100 °C, secondary phases ($SrTa_2O_6$) can be found, which indicates the decomposition of $SrBi_2Ta_2O_9$, attributed to the evaporation of Bi_2O_3. Since higher density can be obtained at relatively low temperatures by SPS, this decomposition can be avoided effectively (Fig. 22).[145]

Recent studies come back to the preparation of dense ceramics of $Bi_4Ti_3O_{12}$ (BIT), starting from nano-sized powders,[146] or even textured BIT ceramics, based on template particles prepared by a molten-salt method (Fig. 23).[147] It can be concluded that: i), the grain size of the material processed by SPS is much finer than that of the pressure-less $Bi_4Ti_3O_{12}$ sintered; and, ii) the SPS is an effective sintering technology to obtain textured BIT ceramics, with anisotropic dielectric properties. The volatilization of bismuth was greatly

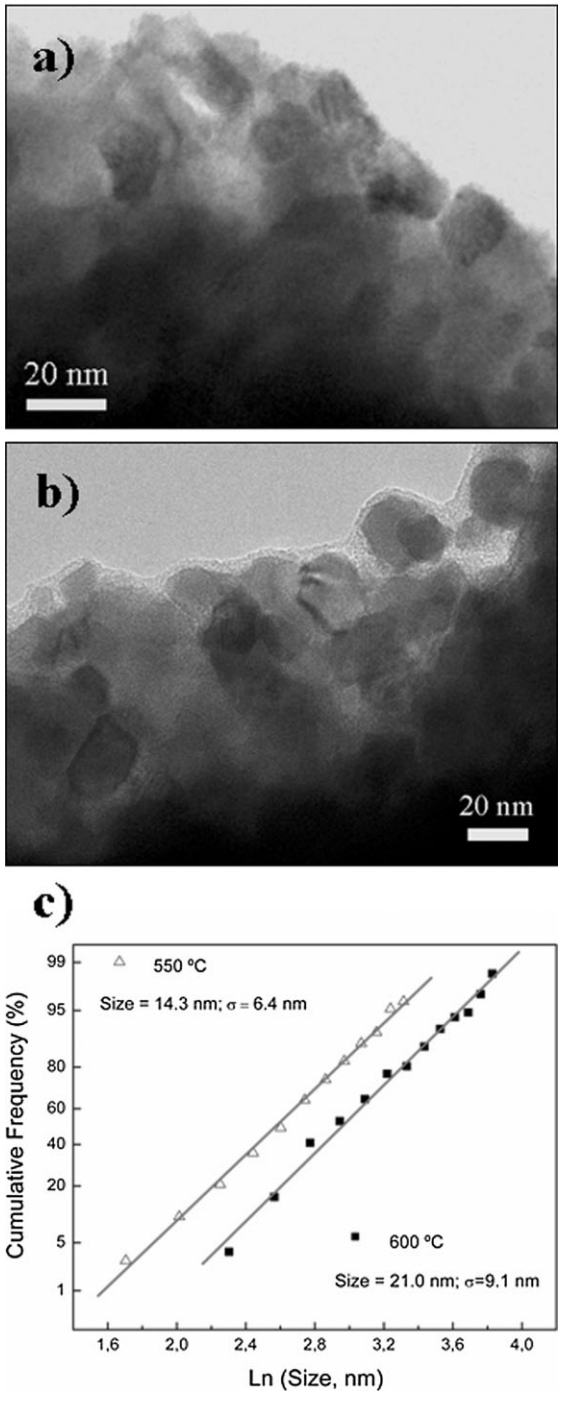

Fig. 21. TEM micrographs of 0.92PZN–0.08PT and ceramics processed by SPS at a) 550 °C, and, b) 600 °C from the powder obtained by mechanosynthesis; and, c) probability plots with the average size and the standard deviation.[137]

restrained during SPS, resulting in suppressed dielectric relaxation and significantly reduced dielectric loss in the ceramics. Moreover Liu et al. carried out a deep study on the SPS behavior of nano-sized BIT and micron-sized $CaBi_2Nb_2O_9$ powders.[148] These authors describe the formation of highly textured compacts, which they suggest are governed by a superplastic deformation-induced directional dynamic ripening mechanism. Moreover, it was shown that, using a

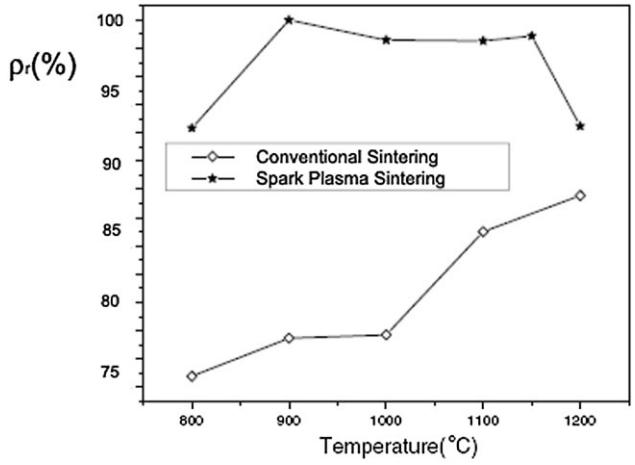

Fig. 22. The curve of densities relative to the theoretical density versus sintering temperatures for the different sintering methods.[145]

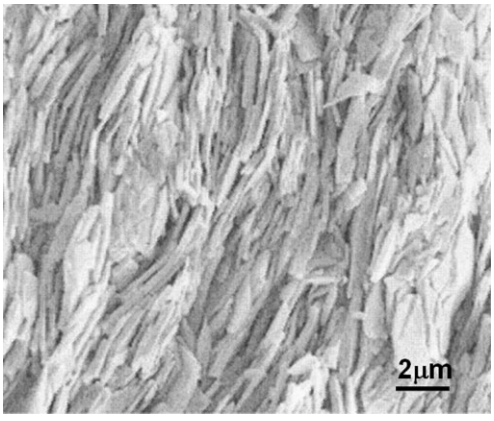

Fig. 23. SEM image of the BIT ceramic processed by SPS at 700 °C for 5 min under a pressure of 25 MPa, applied parallel to the press direction.[147]

nano-sized starting BIT powder, fully dense compacts can be prepared, containing grains of similar size as the starting powder (about 250 nm). This implies that the compaction mainly occurs via grain sliding along grain boundaries.

On the other hand, Yan et al.[149] characterized the ferroelectric, dielectric and piezoelectric properties of $CaBi_2Nb_2O_9$ ceramics, prepared by both conventional sintering and SPS. Their results demonstrate that highly enhanced properties can be obtained in textured ceramic prepared by SPS, with a d_{33} value of nearly three times that of the conventionally obtained ceramic. Finally, this research team also carried out the original processing of $Bi_{3.25}La_{0.75}Ti_3O_{12}$ and $Bi_{3.15}Nd_{0.85}Ti_3O_{12}$ ceramics by dynamic forging during SPS.[150–151] This results in the preparation of grain-oriented ceramics with highly anisotropic ferro-, piezo- and di-electric properties.

3.2.5. Relaxor Tungsten Bronzes

The sintering behavior and electrical properties of piezoelectric ceramic materials, belonging to the families of

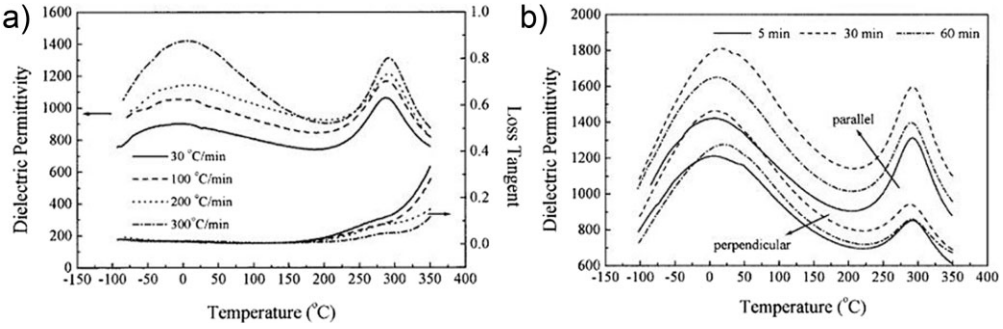

Fig. 24. a) Temperature dependence of the dielectric permittivity and loss tangent of TTB samples sintered at various heating rates. These samples were sintered at 1 200 °C for 5 min and cut from the direction perpendicular to the pressing direction. b) Temperature dependence of the dielectric permittivity of both parallel- and perpendicular-cut specimens as a function of soaking time. These samples were sintered at 1 200 °C with a heating rate of 300 °C min^{-1}.[153]

tetragonal tungsten bronzes (TTB) and with compositions $Sr_{2-x}Ca_xNaNb_5O_{15}$ ($x = 0.1$) and $(Sr_{1.9}Ca_{0.1})_{1-0.5x}Ba_xNaNb_5O_{15}$ (where $x = 0.1$–0.8), were studied, by using the SPS method.[152–154] In these works, Xie et al. conclude that, as expected, the sintering conditions (temperature, heating rate, soaking time, etc.) have a strong influence on the electrical properties of these materials. It is noteworthy that samples sintered at temperatures below 1 200 °C did not show a TTB structure, but a mixture of phases, and were not ferroelectric, while those sintered above 1 200 °C are single TTB phase, with the expected composition and ferroelectric response. Increasing both the heating rate and the soaking time improved the electrical properties (Fig. 24); this is due, among other reasons, to the developed microstructure.

4. Final Remarks on Nanostructuring using Spark Plasma Sintering

Perhaps one of the most interesting application of the SPS technique is the fabrication of nanostructured materials, when nanosized powdered precursors are used. This clear advantage over conventionally employed sintering methods can be attributed to the lower sintering temperature and shorter holding times needed, which allows nearly complete densification with little grain growth to be achieved.

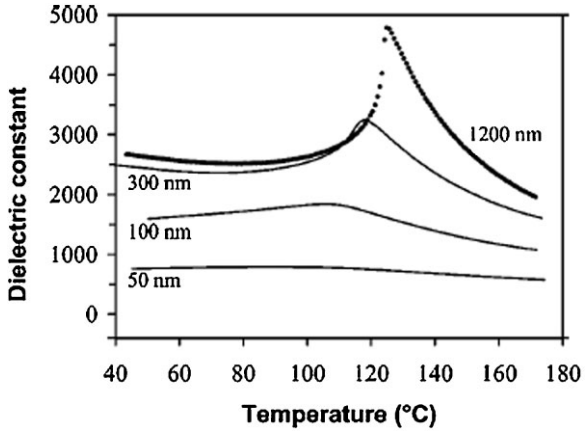

Fig. 25. Relative dielectric constant at 104 Hz of $BaTiO_3$ ceramics with different grain sizes obtained by SPS as a function of temperature.[46]

Few examples of nanostructured-piezoelectric materials have so far been reported, with the exception of those collected in the previous sections. The most studied material is $BaTiO_3$.[96–106] These studies provide evidence of the influence of the size effects on the properties of the materials. Specifically, a systematic investigation of the crystal structure, phase transitions, and permittivity of dense $BaTiO_3$ ceramics, with grain sizes in the range 50–1 200 nm, shows that, as grain size decreases the crystal structure at room temperature becomes progressively less tetragonal and the Curie temperature, obtained from either permittivity or calorimetric measurements, shifts to lower values (Fig. 25).[46] It is worth noting that nanostructured ceramics can only be prepared with the help of the SPS method. The critical grain size corresponding to suppression of ferroelectricity is estimated, in this case, to be 10–30 nm. In addition to the intrinsic size effect, some properties of nanocrystalline ferroelectrics can be also affected by the extrinsic effect of grain boundaries. In particular, the permittivity of $BaTiO_3$ ceramics with grain size below 500 nm seems quite sensitive to the presence of a low permittivity, non-ferroelectric grain boundary layer.

Recently, we reported the first applications of the combination of non-conventional methods of synthesis (mechanosynthesis) and sintering (SPS) for the preparation of nanostructured piezoelectric ceramics, carrying out a comprehensive study of their properties and analyzing the size effects and the applicability limits derived from them. The studies has been focused on the system $(1-x)BiScO_3$–$xPbTiO_3$ (BS–PT) near the morphotropic phase boundary (MPB, near $x = 0.64$)[155,156] and mainly on the phase $0.92PbZn_{1/3}Nb_{2/3}O_3$–$0.08\ PbTiO_3$ (also in the MPB)[49,137] where the results of the electrical characterization indicate that the relaxor state does exist in nanostructured PZN–PT materials with a grain size of 15–20 nm. Similar results were obtained in the case of the $Pb(Zn_{1/3}Nb_{2/3})O_3$–$Pb(Fe_{1/2}Nb_{1/2})O_3$–$PbTiO_3$ system.[157]

Received: February 4, 2009
Revised: April 16, 2009
Published online: June 18, 2009

[1] D. Bernache-Assollant, *Chimie-physique du frittage* (Ed: D. Bernache-Assollant), Hermes FORCERAM Collection, Paris **1993**, Ch. 7.

[2] Z. A. Munir, U. Anselmi-Tamburini, M. Ohyanagi, *J. Mater. Sci.* **2006**, *41*, 763.
[3] G. F. Taylor, *US Patent* **1933**, 1,896,854.
[4] G. D. Cremer, *US Patent* **1944**, 2,355,954.
[5] K. Inoue, *US Patent* **1960**, 2,924,751.
[6] H. Honda, Y. Sanada, K. Inoue, *Carbon* **1964**, *1*, 127.
[7] K. Inoue, *US Patent* **1966**, 3,250,892.
[8] K. Inoue, *US Patent* **1966**, 3,241,956.
[9] S. W. Wang, L. D. Chen, T. Hirai, *J. Mater. Res.* **2000**, *15*, 982.
[10] T. Hungría, M. Algueró, A. B. Hungría, A. Castro, *Chem. Mater.* **2005**, *17*, 6205.
[11] Z. J. Shen, M. Johnsson, Z. Zhao, M. Nygren, *J. Am. Ceram. Soc.* **2002**, *85*, 1921.
[12] M. Tokita, *Mater. Sci. Forum* **1999**, *308–311*, 83.
[13] M. Omori, *Mater. Sci. Eng, A* **2000**, *287*, 183.
[14] D. Zhang, Z. Fu, R. Yuan, J. Guon, *Multiphased Ceramic Materials Processing and Potential*, Vol. *66*(Eds: J. Guo, W.-H. Tua), Springer Series Mate, Berlin **2004**, p. 65.
[15] M. Tokita, *New Ceram.* **1994**, *7*, 63.
[16] D. M. Hulbert, A. Anders, D. V. Dudina, J. Andersson, D. Jiang, C. Unuvar, U. Anselmi-Tamburini, E. J. Lavernia, A. K. Mukherjee, *J. Appl. Phys.* **2008**, *104*, 033305.
[17] G. Jiang, H. Zhuang, W. Li, *Mater. Sci. Eng, A* **2003**, *359*, 377.
[18] E. Olevsky, L. Froyen, *Scr. Mater.* **2006**, *55*, 1175.
[19] S. W. Wang, L. D. Chen, T. Hirai, Y. S. Kang, *J. Mater. Sci. Lett.* **1999**, *18*, 1119.
[20] Y. Makino, *New Ceram.* **1997**, *10*, 39.
[21] H. Tomino, H. Watanabe, Y. Kondo, *J. Jpn. Soc. Powder Metall.* **1997**, *44*, 974.
[22] U. Anselmi-Tamburini, S. Genari, J. E. Garay, Z. A. Munir, *Mater. Sci. Eng, A* **2005**, *394*, 139.
[23] W. Chen, U. Anselmi-Tamburini, J. E. Garay, J. R. Groza, Z. A. Munir, *Mater. Sci. Eng, A* **2005**, *394*, 132.
[24] J. Galy, M. Dolle, T. Hungría, P. Rozier, J. P. Monchoux, *Solid State Sci.* **2008**, *10*, 976.
[25] S. W. Wang, L. D. Chen, T. Hirai, *High-Performance Ceramics 2001, Proceedings* **2002**, *242–244*, 479.
[26] Y. Zhou, K. Hirao, Y. Yamauchi, S. Kanzaki, *Scr. Mater.* **2003**, *48*, 1631.
[27] U. Anselmi-Tamburini, J. E. Garay, Z. A. Munir, A. Tacca, F. Maglia, G. Chiodelli, G. Spinolo, *J. Mater. Res.* **2004**, *19*, 3255.
[28] U. Anselmi-Tamburini, J. E. Garay, Z. A. Munir, A. Tacca, F. Maglia, G. Chiodelli, G. Spinolo, *J. Mater. Res.* **2004**, *19*, 3263.
[29] U. Anselmi-Tamburini, J. E. Garay, Z. A. Munir, *Scr. Mater.* **2006**, *54*, 823.
[30] F. Guillard, A. Allemand, J.-D. Lulewicz, J. Galy, *J. Eur. Ceram. Soc.* **2007**, *27*, 2725.
[31] C. You, D. L. Jiang, S. H. Tan, *J. Am. Ceram. Soc.* **2004**, *87*, 759.
[32] L. Gao, H. Z. Wang, J. S. Hong, H. Miyamoto, S. D. de la Torre, *J. Inorg. Mater.* **1999**, *14*, 55.
[33] J. Wan, R.-G. Duan, A. K. Mukherjee, *Scr. Mater.* **2005**, *53*, 663.
[34] L. J. Wang, W. Jiang, L. D. Chen, S. Q. Bai, *J. Am. Ceram. Soc.* **2004**, *87*, 1157.
[35] Y. Zheng, S. Wang, M. You, H. Tan, W. Xiong, *Mater. Chem. Phys.* **2005**, *92*, 64.
[36] B. Basu, J. H. Lee, D. Y. Kim, *J. Am. Ceram. Soc.* **2004**, *87*, 317.
[37] S. H. Shim, K. Niihara, K. H. Auh, K. B. Shim, *J. Microsc.* **2002**, *205*, 238.
[38] V. Medri, F. Monteverde, A. Balbo, A. Bellosi, *Adv. Eng. Mater.* **2005**, *7*, 159.
[39] Z. J. Shen, M. Nygren, *J. Mater. Chem.* **2001**, *11*, 204.
[40] S. Kawano, J. Takahashi, S. Shimada, *J. Eur. Ceram. Soc.* **2004**, *24*, 309.
[41] Y. Xiong, Z. Y. Fu, H. Wang, Y. C. Wang, Q. J. Zhang, *Mater. Sci. Eng, B* **2005**, *123*, 57.
[42] B. Prawara, H. Yara, Y. Miyagi, T. Fukushima, *Surf. Coat. Technol.* **2003**, *162*, 234.
[43] L. Gao, J. S. Hong, S. Torre, *J. Eur. Ceram. Soc.* **2000**, *20*, 2149.
[44] T. Takeuchi, E. Betourne, M. Tabuchi, H. Kageyama, *J. Mater. Sci.* **1999**, *34*, 917.
[45] J. Liu, Z. J. Shen, M. Nygren, Y. M. Kan, P. L. Wang, *J. Eur. Ceram. Soc.* **2004**, *24*, 3233.
[46] Z. Zhao, V. Buscaglia, M. Viviani, M. T. Buscaglia, L. Mitoseriu, A. Testino, M. Nygren, M. Johnsson, P. Nanni, *Phys. Rev. B* **2004**, *70*, 024107.
[47] T. Takeuchi, M. Tabuchi, I. Kondoh, N. Tamari, H. Kageyama, *J. Am. Ceram. Soc.* **2000**, *83*, 541.
[48] T. Hungría, M. Algueró, A. Castro, *J. Am. Ceram. Soc.* **2007**, *90*, 2122.
[49] M. Algueró, T. Hungría, H. Amorín, J. Ricote, J. Galy, A. Castro, *Small* **2007**, *3*, 1906.
[50] J. S. Lee, C. M. Chang, Y. I. Lee, J. H. Lee, S. H. Hong, *J. Am. Ceram. Soc.* **2004**, *87*, 305.
[51] Z. J. Shen, E. Adolfsson, M. Nygren, L. Gao, H. Kawaoka, K. Niihara, *Adv. Mater.* **2001**, *13*, 214.
[52] J. L. Xu, K. A. Khor, Y. W. Gu, R. Kumar, P. Cheang, *Biomaterials* **2005**, *26*, 2197.
[53] T. Grosdidier, G. Ji, S. Launois, *Scr. Mater.* **2007**, *57*, 525.
[54] J. C. Ye, L. Ajdelsztajn, J. M. Schoenung, *Metall. Mater. Trans. A* **2006**, *37A*, 2569.
[55] G. Molenat, M. Thomas, J. Galy, A. Couret, *Adv. Eng. Mater.* **2007**, *9*, 667.
[56] A. Couret, G. Molenat, J. Galy, M. Thomas, *Intermetallics* **2008**, *16*, 1134.
[57] T. Grosdidier, G. Ji, F. Bernard, E. Gaffet, Z. A. Munir, S. Launois, *Intermetallics* **2006**, *14*, 1208.
[58] H. Feng, Q. Meng, Y. Zhou, D. Jia, *Mater. Sci. Eng, A* **2005**, *397*, 92.
[59] A. Bellosi, F. D. Monteverde, D. Sciti, *Int. J. Appl. Ceram. Tech.* **2006**, *3*, 32.

[60] Z. J. Shen, Z. Zhao, H. Peng, M. Nygren, *Nature* **2002**, *417*, 266.
[61] Z. J. Shen, H. Peng, M. Nygren, *Adv. Mater.* **2003**, *15*, 1006.
[62] D. T. Jiang, D. M. Hulbert, J. D. Kuntz, U. Anselmi-Tamburini, A. K. Mukherjee, *Mater. Sci. Eng, A* **2007**, *463*, 89.
[63] J. Galy, *Private Communication* **2007**.
[64] P. Greil, *Adv. Mater.* **2002**, *14*, 709.
[65] J. Galy, *Private Communication* **2007**.
[66] L. Gao, Z. J. Shen, H. Miyamoto, M. Nygren, *J. Am. Ceram. Soc.* **1999**, *82*, 1061.
[67] C. K. Kim, H. S. Lee, S. Y. Shin, J. C. Lee, D. H. Kim, S. Lee, *Mater. Sci. Eng, A* **2006**, *429*, 348.
[68] Y. S. Ding, S. M. Dong, Z. R. Huang, D. L. Jiang, *Ceram. Int.* **2007**, *33*, 101.
[69] R. Poyato, A. L. Vasiliev, N. P. Padture, H. Tanaka, T. Nishimura, *Nanotechnology* **2006**, *17*, 1770.
[70] L. J. Wang, T. Wu, W. Jiang, J. L. Li, L. D. Chen, *J. Am. Ceram. Soc.* **2006**, *89*, 1540.
[71] J. F. Zhang, L. J. Wang, L. Shi, W. Jiang, L. D. Chen, *Scr. Mater.* **2007**, *56*, 241.
[72] U. Anselmi-Tamburini, Y. Kodera, M. Gasch, C. Unuvar, Z. A. Munir, M. Ohyanagi, S. M. Johnson, *J. Mater. Sci.* **2006**, *41*, 3097.
[73] J. Galy, J. P. Monchoux, *J. Mater. Sci.* **2008**, *43*, 6391.
[74] T. Hiroshima, K. Tanaka, T. Kimura, *J. Am. Ceram. Soc.* **1996**, *79*, 3235.
[75] H. Y. Lee, R. Freer, *J. Appl. Phys.* **1997**, *81*, 376.
[76] K. Nagata, Y. Kawatani, K. Okazaki, *Jpn. J. Appl. Phys.* **1983**, *22*, 1353.
[77] N. S. VanDamme, A. E. Sutherland, L. Jones, K. Bridger, S. R. Winzer, *J. Am. Ceram. Soc.* **1991**, *74*, 1785.
[78] S. Nishiwaki, J. Takahashi, K. Kodaira, *Jpn. J. Appl. Phys.* **1994**, *33*, 5477.
[79] R. E. Jaeger, L. Egreton, *J. Am. Ceram. Soc.* **1962**, *45*, 209.
[80] G. H. Haertling, *J. Am. Ceram. Soc.* **1967**, *50*, 329.
[81] P. Papet, J. P. Dougherty, T. R. Shrout, *J. Mater. Res.* **1990**, *5*, 2902.
[82] C. A. Randall, A. D. Hilton, D. J. Barber, T. R. Shrout, *J. Mater. Res.* **1993**, *8*, 880.
[83] T. R. Shrout, U. Kumar, M. Megherhi, N. Yang, *Ferroelectrics* **1987**, *76*, 479.
[84] C. A. Randall, N. Kim, J. P. Kucera, W. Cao, T. R. Shrout, *J. Am. Ceram. Soc.* **1998**, *81*, 677.
[85] H. Yamada, *J. Euro. Ceram. Soc.* **1999**, *19*, 1053.
[86] Z. P. Xie, Z. L. Gui, L. T. Li, T. Su, Y. Huang, *Mater. Lett.* **1998**, *36*, 191.
[87] M. H. Lente, A. L. Zanin, S. B. Assis, I. A. Santos, J. A. Eiras, D. Garcia, *J. Eur. Ceram. Soc.* **2004**, *24*, 1529.
[88] M. R. Cox, *J. Mater. Sci. Lett.* **2000**, *19*, 333.
[89] G. H. Haertling, *J. Am. Ceram. Soc.* **1971**, *54*, 303.
[90] G. S. Snow, *J. Am. Ceram. Soc.* **1973**, *56*, 91.
[91] Y. Abe, K. Kakegawa, H. Ushijima, Y. Watanabe, Y. Sasaki, *J. Am. Ceram. Soc.* **2002**, *85*, 473.
[92] J. Choi, J. Ryu, H. Kim, *J. Am. Ceram. Soc.* **2001**, *84*, 1465.
[93] G. Arlt, D. Hennings, G. DeWith, *J. Appl. Phys.* **1985**, *58*, 1619.
[94] B. Li, X. Wang, L. Li, H. Zhou, X. Liu, X. Han, Y. Zhang, X. Qi, X. Deng, *Mater. Chem. Phys.* **2004**, *83*, 23.
[95] K. Oonishi, T. Morohashi, K. Uchino, *J. Ceram. Soc. Jpn.* **1989**, *97*, 473.
[96] T. Takeuchi, M. Tabuchi, H. Kageyama, Y. Suyama, *J. Am. Ceram. Soc.* **1999**, *82*, 939.
[97] T. Takeuchi, Y. Suyama, D. C. Sinclair, H. Kageyama, *J. Mater. Sci.* **2001**, *36*, 2329.
[98] T. Takeuchi, C. Capiglia, N. Balakrishnan, T. Takeda, H. Kageyama, *J. Mater. Res.* **2002**, *17*, 575.
[99] B. R. Li, X. H. Wang, M. M. Cai, L. F. Hao, L. T. Li, *Mater. Chem. Phys.* **2003**, *82*, 173.
[100] W. L. Luan, L. Gao, H. Kawaoka, T. Sekino, K. Niihara, *Ceram. Int.* **2004**, *30*, 405.
[101] M. T. Buscaglia, V. Buscaglia, M. Viviani, J. Petzelt, M. Savinov, L. Mitoseriu, A. Testino, P. Nanni, C. Harnagea, Z. Zhao, M. Nygren, *Nanotechnology* **2004**, *15*, 1113.
[102] V. Buscaglia, M. T. Buscaglia, M. Viviani, T. Ostapchuk, I. Gregora, J. Petzelt, L. Mitoseriu, P. Nanni, A. Testino, R. Calderone, C. Harnagea, Z. Zhao, M. Nygren, *J. Eur. Ceram. Soc.* **2005**, *25*, 3059.
[103] R. Licheri, S. Fadda, R. Orru, G. Cao, V. Buscaglia, *J. Eur. Ceram. Soc.* **2007**, *27*, 2245.
[104] X. Y. Deng, X. H. Wang, H. Wen, L. L. Chen, L. Chen, L. T. Li, *Appl. Phys. Lett.* **2006**, *88*, 52905.
[105] H. Maiwa, *Jpn. J. Appl. Phys.* **2008**, *47*, 7646.
[106] X. Y. Deng, X. H. Wang, H. Wen, A. G. Kang, Z. L. Gui, L. T. Li, *J. Am. Ceram. Soc.* **2006**, *89*, 1059.
[107] H. Maiwa, *J. Mater. Sci.* **2008**, *43*, 6385.
[108] B. Su, J. Y. He, B. L. Cheng, T. W. Button, J. Liu, Z. Shen, M. Nygren, *Integrated Ferroelectrics* **2004**, *61*, 117.
[109] J. Liu, Z. J. Shen, M. Nygren, *Ferroelectrics* **2005**, *319*, 335.
[110] J. Liu, Z. J. Shen, M. Nygren, B. Su, T. W. Button, *J. Am. Ceram. Soc.* **2006**, *89*, 2689.
[111] C. Shen, Q. F. Liu, Q. Liu, *Mater. Lett.* **2004**, *58*, 2302.
[112] T. Takeuchi, H. Kageyama, *J. Mater. Res.* **2003**, *18*, 1809.
[113] Q. Huang, L. Gao, *Appl. Phys. Lett.* **2005**, *86*, 23104.
[114] Q. Huang, L. Gao, Y. Q. Liu, J. Sun, *J. Mater. Chem.* **2005**, *15*, 1995.
[115] S. Rattanachan, Y. Miyashita, Y. Mutoh, *Sci. Technol. Adv. Mater.* **2005**, *6*, 704.
[116] G. D. Zhan, J. Kuntz, J. L. Wan, J. Garay, A. K. Mukherjee, *Mater. Sci. Eng, A* **2003**, *356*, 443.
[117] M. T. Buscaglia, M. Viviani, Z. Zhao, V. Buscaglia, P. Nanni, *Chem. Mater.* **2006**, *18*, 4002.
[118] T. Hungría, M. Algueró, A. Castro, *Chem. Mater.* **2006**, *18*, 5370.
[119] R. P. Wang, R. J. Xie, T. Sekiya, Y. Shimojo, Y. Akimune, N. Hirosaki, M. Itoh, *Jpn. J. Appl. Phys.* **2002**, *41*, 7119.
[120] T. Wada, K. Tsuji, T. Saito, Y. Matsuo, *Jpn. J. Appl. Phys.* **2003**, *42*, 6110.
[121] R. P. Wang, R. J. Xie, T. Sekiya, Y. Shimojo, *Mater. Res. Bull.* **2004**, *39*, 1709.

[122] B. P. Zhang, J. F. Li, K. Wang, H. L. Zhang, *J. Am. Ceram. Soc.* **2006**, *89*, 1605.
[123] J. F. Li, K. Wang, B. P. Zhang, L. M. Zhang, *J. Am. Ceram. Soc.* **2006**, *89*, 706.
[124] R. P. Wang, R. J. Xie, K. Hanada, K. Matsusaki, H. Bando, M. Itoh, *Phys. Status Solidi A* **2005**, *202*, R57.
[125] J. Kano, K. Sasanuma, S. Tsukada, S. Kojima, R. Wang, K. Hanada, K. Matsusaki, H. Bando, *Ferroelectrics* **2007**, *347*, 55.
[126] K. Sasanuma, S. Tsukada, J. Kano, S. Kojima, R. Wang, K. Hanada, K. Matsusaki, H. Bando, *Ferroelectrics* **2007**, *348*, 508.
[127] K. Kakegawa, Y. Kawai, Y. J. Wu, N. Uekawa, Y. Sasaki, *J. Am. Ceram. Soc.* **2004**, *87*, 541.
[128] Y. J. Wu, N. Uekawa, K. Kakegawa, Y. Sasaki, *Mater. Lett.* **2002**, *57*, 771.
[129] J. K. Park, U. J. Chung, N. M. Hwang, D. Y. Kim, *J. Am. Ceram. Soc.* **2001**, *84*, 3057.
[130] K. P. Chen, C. W. Li, X. W. Zhang, Y. Huang, *Mater. Lett.* **2002**, *57*, 20.
[131] J. K. Park, U. J. Chung, D. Y. Kim, *J. Electroceram.* **2006**, *17*, 509.
[132] R. Z. Zuo, T. Granzow, D. C. Lupascu, J. Rodel, *J. Am. Ceram. Soc.* **2007**, *90*, 1101.
[133] Y. Shimojo, R. Wang, Y. J. Shan, H. Izui, M. Taya, *Ceram. Int.* **2008**, *34*, 1449.
[134] K. Kakegawa, N. Uekawa, Y. J. Wu, Y. Sasaki, *Mater. Sci. Eng, B* **2003**, *99*, 11.
[135] Y. J. Wu, N. Uekawa, Y. Sasaki, K. Kakegawa, Y. Sasaki, *J. Am. Ceram. Soc.* **2002**, *85*, 1988.
[136] Y. J. Wu, R. Kimura, N. Uekawa, K. Kakegawa, Y. Sasaki, *Jpn. J. Appl. Phys.* **2002**, *41*, L219.
[137] T. Hungría, H. Amorín, J. Galy, J. Ricote, M. Algueró, A. Castro, *Nanotechnology* **2008**, *19*, 155609.
[138] L. J. Zhou, Z. Zhao, A. Zimmermann, F. Aldinger, M. Nygren, *J. Am. Ceram. Soc.* **2004**, *87*, 606.
[139] L. J. Zhou, G. Rixecker, F. Aldinger, *J. Am. Ceram. Soc.* **2006**, *89*, 3868.
[140] Y. J. Wu, J. Li, R. Kimura, N. Uekawa, K. Kakegawa, *J. Am. Ceram. Soc.* **2005**, *88*, 3327.
[141] K. P. Chen, C. W. Li, C. Lei, X. W. Zhang, Y. Huang, *J. Mater. Sci. Lett.* **2002**, *21*, 1785.
[142] J. Takahashi, S. Kawano, S. Shimada, K. Kageyama, *Jpn. J. Appl. Phys.* **1999**, *38*, 5493.
[143] Y. J. Wu, N. Uekawa, K. Kakegawa, *Mater. Lett.* **2003**, *57*, 4088.
[144] H. X. Yan, H. T. Zhang, R. Ubic, M. Reece, J. Liu, Z. J. Shen, *J. Mater. Sci.: Mater. Electron.* **2006**, *17*, 657.
[145] B. R. Li, X. H. Wang, X. Q. Han, X. W. Qi, L. T. Li, *J. Mater. Sci.* **2004**, *39*, 2621.
[146] Y. M. Kan, P. L. Wang, T. Xu, G. J. Zhang, D. S. Yan, Z. J. Shen, Y. B. Cheng, *J. Am. Ceram. Soc.* **2005**, *88*, 1631.
[147] J. J. Hao, X. H. Wang, R. Z. Chen, Z. L. Gui, L. T. Li, *J. Am. Ceram. Soc.* **2004**, *87*, 1404.
[148] J. Liu, Z. J. Shen, M. Nygren, Y. M. Kan, P. L. Wang, *J. Eur. Ceram. Soc.* **2006**, *26*, 3233.
[149] H. X. Yan, H. T. Zhang, R. Ubic, M. J. Reece, J. Liu, Z. J. Shen, Z. Zhang, *Adv. Mater.* **2005**, *17*, 1261.
[150] J. Liu, Z. Shen, H. Yan, M. J. Reece, Y. Kan, P. Wang, *J. Appl. Phys.* **2007**, *102*, 104107.
[151] H. Zhang, H. Yan, X. Zhang, M. J. Reece, J. Liu, Z. Shen, Y. Kan, P. Wang, *Mater. Sci. Eng, A* **2008**, *475*, 92.
[152] R. J. Xie, Y. Akimune, R. P. Wang, K. Matsuo, T. Sugiyama, N. Hirosaki, *J. Am. Ceram. Soc.* **2002**, *85*, 2725.
[153] R. J. Xie, Y. Akimune, R. P. Wang, N. Hirosaki, *J. Am. Ceram. Soc.* **2002**, *85*, 2731.
[154] R. J. Xie, Y. Akimune, R. P. Wang, N. Hirosaki, T. Nishimura, *Jpn. J. Appl. Phys.* **2003**, *42*, 7404.
[155] T. Hungría, H. Amorín, M. Algueró, A. Castro, J. M. Vicente, J. Ricote, J. Galy, *2nd Workshop Processing and Characterization of Nanostructured Systems*, Brussels, Belgium **2006**.
[156] M. Algueró, H. Amorín, T. Hungría, J. Galy, A. Castro, *Appl. Phys. Lett.* **2009**, *94*, 012902.
[157] H. Amorín, R. Jiménez, T. Hungría, A. Castro, M. Algueró, *Appl. Phys. Lett.* **2009**, *94*, 152902.

